Spin current in topologically trivial and nontrivial noncentrosymmetric superconductors

Chi-Ken Lu[1,2,*] and Sungkit Yip[1]
[1]*Institute of Physics, Academia Sinica, Nankang, Taipei 115, Taiwan*
[2]*Department of Physics, Simon Fraser University, 8888 University Drive, Burnaby, British Columbia, Canada V5A 1S6*
(Received 19 April 2010; revised manuscript received 22 June 2010; published 1 September 2010)

We study theoretically the surface of time-reversal-symmetric, noncentrosymmetric superconductor with mixed singlet and triplet order parameters. A pair of counterpropagating subgap quasiparticle surface bound states with opposite spin projections are obtained in the nontrivial Z_2 case where the triplet component is larger than the singlet one, contributing to a spin current with out-of-plane spin projection. In contrast to the pure p-wave cases, these subgap states do not have fixed spin projections, which, however, depend on the momenta along the surface. In the trivial Z_2 case where the singlet order parameter is larger, no subgap surface bound states show up. In both cases, there is also a finite contribution to the spin current from the continuum states with energies between the two gaps. The method for obtaining the quasiclassical Green's functions associated with the noncentrosymmetric superconductors is also presented.

DOI: 10.1103/PhysRevB.82.104501 PACS number(s): 74.45.+c, 74.20.Rp, 72.25.−b

I. INTRODUCTION

How to manipulate spin in condensed-matter system has been the main challenge for both experimentalists and theorists in this community. Recently, the predictions[1–3] and observations[4–7] of topological insulators (TIs) with time-reversal symmetry (TRS), such as HgTe/(Hg,Ce)Te semiconductor wells,[4] $Bi_{1-x}Sb_x$,[5] Bi_2Se_3,[6] and Bi_2Te_3,[7] inspire a great deal of interest in both the application and the fundamental research ends. The main feature of a TI is a pair of counterpropagating edge states with opposite spin projections developed out of a gapped band structure, very much like the edge states in the integer Quantum Hall case except that the TRS is broken in the latter case. In the language of homotopy, the mapping from the momentum space to the Hamiltonian can be smoothly deformed into either one of the two distinct elements in the so-called Z_2 class associated with the trivial and nontrivial TIs. This pair of surface bound states contributes to a spin current near the surface of a TI.[8]

The concept of TI can also be generalized to superconductors (SCs). A simple example is the [two-dimensional (2D)] p-wave superconductor with its order parameter given by $\vec{d}=k_x\hat{y}-k_y\hat{x}$. We can see explicitly from the order parameter $\propto[(k_x-ik_y)|\uparrow\uparrow\rangle+(k_x+ik_y)|\downarrow\downarrow\rangle]$ that the Cooper pairs with down (up) spins have a counterclockwise (clockwise) motion. This state is clearly time-reversal symmetric. Each species is in an axial state, considered in, e.g., Refs. 9 and 10, with the phase of the Cooper pair wave function advances (decreases) by 2π when the angle of the momentum direction advances by the same angle. Considering the surface of this superconductor adjacent to vacuum, the incident and reflected quasiparticles see an order parameter with a different phase factor, analogous to the case of a Josephson junction. A pair of surface bound states with opposite spin projections propagate in opposite directions, generating no charge but finite spin current, as in the case of a topological insulator. Moreover, straightforward generalization of the results of Refs. 9 and 10 implies that a singly quantized vortex of this superconductor possesses a pair of zero-energy Majorana states inside its vortex core. In contrast, the order parameter of an s-wave singlet superconductor do not change sign over the Fermi surface. No surface bound states are topologically required and the superconductor thus belongs to trivial class.

For noncentrosymmetric SCs (NcSCs), such as the compounds $CePt_3Si$,[11] Li_2Pt_3B,[12] and $CeRhSi_3$,[13] and the 2D electron gas between two insulating layers,[14] complication arises due to the presence of parity-broken spin-orbital interaction and the singlet-triplet mixed superconducting order parameters.[15] For example, for a system with no up-down reflection symmetry, the s-wave singlet order parameter Δ_s and the triplet order parameters Δ_p with the d vector given by $(k_x\hat{y}-k_y\hat{x})$ would naturally mix since they are of the *same* symmetry.[16] Alternatively, the two Fermi surfaces with opposite helicities can be associated with two different superconducting gaps as a result of the broken-inversion symmetry.[17] Nevertheless, the topological classifications still can be deduced from the existence of zero-energy vortex bound states[18] or the surface bound states.[19] These studies reveal that only the relative signs of the pairing terms on the opposite-helicity bands matter for the topology, which can also be shown by more explicit topological arguments.[20,21] NcSC with opposite signs of pairing on the two bands resembles the pure p-wave triplet superconductor in that a pair of topologically protected zero energy or surface bound states reside within the vortex core or at the surface, respectively, while these topological bound states do not exist at all in the NcSC with same sign of pairing, which resembles the pure s-wave singlet SC.

In this paper we shall consider in more detail the surface of a NcSC, as shown in Fig. 1, as a function of the singlet Δ_s and triplet Δ_p order parameters. For simplicity, here we would not consider the dispersion along the z axis (or effectively 2D) nor the splitting of the Fermi surfaces due to spin-orbit interactions. The absence of spin-orbital coupling may, in fact, correspond to a narrowly accessible physical regime in mixed-parity superconductivity.[22] Our simplification, however, does not affect the main physics that we would like to explain in this paper. Comments on this aspect will be given later.

For the present geometry, there is no xy-plane reflection symmetry whereas the time-reversal symmetry and the

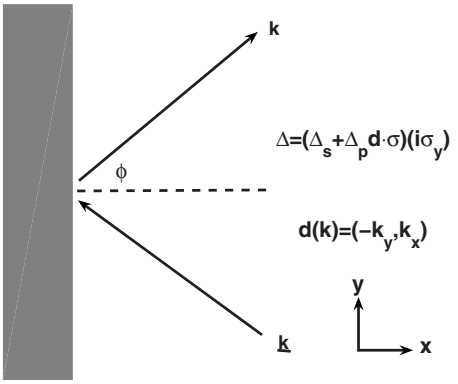

FIG. 1. The interface between vacuum (gray) and a noncentrosymmetric superconductor (white) with singlet-triplet mixed order parameter specified by text. The directions are defined by the shown axis. The quasicparticle is incident from the lower right of xy plane along the path denoted by $\underline{k}$. ϕ is the reflection angle between the x axis and the outgoing path $\hat{k}$.

xz-plane reflection symmetry are left intact. Following the same symmetry arguments as in our previous paper,[23] the magnetization along any directions automatically vanish due to the time-reversal invariance. However, the spin currents J_y^z, J_y^x, and J_x^y can, in principle, be allowed. We shall examine whether these spin currents are finite.

In the pure p-wave case ($|\Delta_s|=0$), the bound states have their spins quantized parallel or antiparallel to the z axes. Only J_y^z is nonzero.[23,24] We would examine what happen to these states when Δ_s is finite, especially their spin directions. We shall see that the spins are no longer polarized along z in the general case. In the context of topological superconductor, the parity-mixed order parameters with $|\Delta_p|>|\Delta_s|$ belong to the nontrivial Z_2 class,[18–20] and the pair of surface bound states with opposite spin projections propagating in opposite directions still exist. These surface bound states can, in principle, be detected by tunneling conductance, which has now been investigated in great detail theoretically.[19,25,26] We shall, however, concentrate on the spin currents in this paper. These surface states can still generate the spin currents J_y^z (and, in principle, also J_y^x, but see below). However, as we shall see, this is *not* the only contribution. For the case of $|\Delta_s|>|\Delta_p|$, the superconductor belongs to the trivial category and it is expected that the surface bound states do not survive. An immediate question is, at the transition point for $|\Delta_p|=|\Delta_s|$, whether the spin current drops to zero abruptly, signaling the transition of topology, or it is smoothly decreasing toward zero, coinciding with the pure s-wave case only when Δ_p vanishes. In the following, we shall consider the above questions by evaluating quantities such as the momentum- and spin-resolved densities of states and the spin current of the NcSC with varying ratio $|\Delta_p|/|\Delta_s|$. We find that nonzero spin current J_y^z is dictated only by the broken symmetry and can be finite for both the topological trivial and nontrivial superconductors. The contribution to this spin current turns out to arise also from nontopological *continuum* states with energies between the two gaps $|\Delta_p \pm \Delta_s|$. These states are present in both the topological trivial and nontrivial superconductors, and they are not required by topology. (We recall here the analogous situation that a finite spin Hall conductivity is possible from the Kubo formula[27] yet the model can belong to the topologically trivial Z_2 class[3]). Lastly, though, in principle, J_y^x and J_x^y are allowed by symmetry, we found that they vanish within our calculations.

II. QUASICLASSICAL GREEN'S FUNCTION ASSOCIATED WITH NcSC

Now we use the quasiclassical Green's functions to investigate the surface of a clean NcSC. Here we shall employ the so-called exploding and decaying tricks,[28–30] which is related to the projector formalism initiated by Shelankov.[31] This method is different from the approach which employs the Riccati transformation.[32] The Matsubara Green's function $\hat{g}(\hat{k},\epsilon_n,R)$ in spin and particle-hole space satisfies the Eilenberger equation[33]

$$[i\epsilon_n\tau_3-\hat{\Delta},\hat{g}]+i\vec{v}_f\cdot\vec{\nabla}_R\hat{g}=0 \tag{1}$$

with the normalization condition

$$\hat{g}^2=-\pi^2\hat{1}. \tag{2}$$

Here ϵ_n and $\hat{k}$ denote the Matsubara frequency and momentum direction associated with the quasiparticles, respectively. R represents the spatial position. The set of matrix $\{1,\vec{\tau}\}$ is used in the particle-hole sector while $\{1,\vec{\sigma}\}$ serve for the usual spins. In this representation, the 4×4 pairing order parameter can be written as

$$\hat{\Delta}=\begin{pmatrix}0 & \underline{\Delta}\\ -\underline{\Delta}^\dagger & 0\end{pmatrix}, \tag{3}$$

where the 2×2 matrix $\underline{\Delta}=[\Delta_s+\Delta_p\vec{d}(\vec{k})\cdot\vec{\sigma}](i\sigma_y)$ in the usual spin representation. Here $\hat{\bullet}$ and $\underline{\bullet}$ are to denote the 4×4 and 2×2 matrices, respectively. The triplet order parameter we consider is of Rashba form $\vec{d}=(-k_y,k_x)$. Δ_s and Δ_p can be both taken real since we assumed TRS. Without loss of generality, they will both be assumed positive. There are two energy gaps, $|\Delta_p\pm\Delta_s|$, associated with the quasiparticles in the superconducting states.[34] One should also note that we have not included the spin-orbital coupling term which may arise from the lack of inversion symmetry in the normal state. Therefore, only one Fermi surface and its associated Fermi velocity v_F are needed. Qualitative effects of including the spin-orbital coupling will be discussed later in the paper. For simplicity, we shall also ignore the spatial variations in the order parameters $\Delta_{s,p}$.

We consider the geometry shown in Fig. 1. The incoming and reflecting quasiparticles have the momentum $\underline{k}$ and k, respectively. Here $k_x>0$ and $\underline{k}_x<0$. We label positions along the quasiparticle path consisting of each pairs of $\hat{k}$ and $\underline{\hat{k}}$ by u with $u>0$ ($u<0$) labels the part for $\hat{k}(\underline{\hat{k}})$. The quasiclassical Green's function at the surface $\hat{g}(0)$ can be obtained in terms of the decaying and exploding solutions to Eq. (1) (cf. Ref. 30)

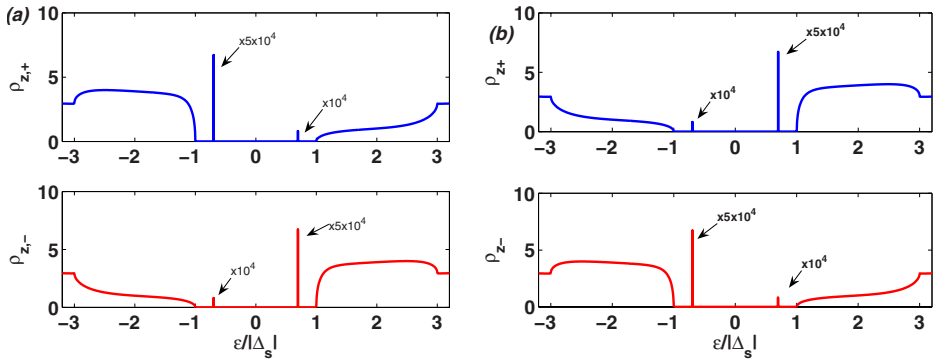

FIG. 2. (Color online) Momentum- and spin-resolved surface densities of states $\rho_{z,\pm}$ in unit of $\frac{N_F}{\pi}$ with $|\Delta_p|=2|\Delta_s|$. (a) $\phi=\frac{\pi}{6}$. (b) $\phi=-\frac{\pi}{6}$. Note that the upper (lower) plot in (a) is identical to the lower (upper) one in (b) due to the time-reversal symmetry. The numerical values associated with the subgap peaks are related to the small imaginary number $\delta=10^{-6}$ we used in the transformation $i\epsilon_n \to \epsilon+i\delta$, which is also true in Fig. 3.

$$\hat{g}(0) = -i\pi[\hat{A}(k),\hat{B}(\underline{k})]\{\hat{A}(k),\hat{B}(\underline{k})\}^{-1}, \tag{4}$$

where the matrix $\hat{A}=\hat{a}^{++}+\hat{a}^{--}$ and $\hat{B}=\hat{b}^{++}+\hat{b}^{--}$. Below the four matrix solutions $\hat{a}^{\pm\pm}$ and $\hat{b}^{\pm\pm}$ are explicitly shown

$$\hat{a}^{\pm\pm} = \left(\frac{1 \pm \hat{d}\cdot\hat{\sigma}\tau_3}{2}\right)[-i|\Delta_\pm|^2\tau_3 - i(\alpha_\pm + \epsilon_n) \times (\Delta_s + \Delta_p\hat{d}\cdot\vec{\sigma})\sigma_y\tau_+ + i(\alpha_\pm - \epsilon_n)\sigma_y(\Delta_s^* + \Delta_p^*\hat{d}\cdot\vec{\sigma})\tau_-], \tag{5}$$

$$\hat{b}^{\pm\pm} = \left(\frac{1 \pm \hat{d}\cdot\hat{\sigma}\tau_3}{2}\right)[i|\Delta_\pm|^2\tau_3 - i(\alpha_\pm - \epsilon_n) \times (\Delta_s + \Delta_p\hat{d}\cdot\vec{\sigma})\sigma_y\tau_+ + i(\alpha_\pm + \epsilon_n)\sigma_y(\Delta_s^* + \Delta_p^*\hat{d}\cdot\vec{\sigma})\tau_-], \tag{6}$$

where the notation we used for the three 4×4 matrix $\hat{\sigma} \equiv (\sigma_x,\sigma_y\tau_3,\sigma_z)$ should be noticed. The parameters $\alpha_\pm = \sqrt{\epsilon_n^2+|\Delta_\pm|^2}$, where $\Delta_\pm=\Delta_s\pm\Delta_p$. More details can be found in Appendix.

III. SURFACE BOUND STATES AND SPIN CURRENTS

Equipped with Eqs. (4)–(6), we are ready to investigate the surface bound states and spin currents at the surface. We do so by evaluating the spin- and momentum-resolved densities of states along different spin projection directions. For example, for a given momentum, the density of states at the surface for spins along positive (negative) z axis is given by $\rho_{z\pm}(\epsilon)=-\frac{N_F}{\pi}\mathrm{Im\ Tr}[\frac{1\pm\sigma_z}{2}\underline{g}^{\mathrm{R}}(\hat{k},\epsilon;x=0)]$, where $\underline{g}^{\mathrm{R}} = \underline{g}|_{i\epsilon_n\to\epsilon+i\delta,\epsilon_n>0}$ is the retarded Green's function. Similar formulas apply by replacing z with the other corresponding directions. Here $\underline{g}$ is the 2×2 matrix in spin space given by the upper left block of $\hat{g}$ in the Nambu space.

We shall show the results for representative cases of nontrivial Z_2 with $|\Delta_p/\Delta_s|=2$ and trivial Z_2 with $|\Delta_p/\Delta_s|=1/2$. Figure 2 shows the spin-resolved density of states $\rho_{z,\pm}$ with $\phi=\pm\frac{\pi}{6}$ and $|\Delta_p/\Delta_s|=2$. The momentum $k_y=k_F\sin\phi$ is a good quantum number as a result of the translational invariance along $\hat{y}$. The peaks below the gap indicate the surface bound-state energy corresponding to

$$\det[\{\hat{A}(k),\hat{B}(\underline{k})\}]|_{i\epsilon_n\to\epsilon+i\delta}=0. \tag{7}$$

In the case of pure p wave ($\Delta_s=0$), the bound-state spectrum is given by $E_{S_z=\pm}(k_y)=\mp|\Delta_p|\sin\phi$.[23,24] In this limit these surface quasiparticles have a fixed spin orientation. Hence $\rho_{z\pm}(\epsilon)$ consists of a single delta function peak at $\epsilon=\mp|\Delta_p|\sin\phi$. In contrast, in Figs. 2(a) and 2(b), we find two subgap peaks, though with large differences in height. These indicate that the quasiparticles in the NcSC are no longer eigenstates of S_z in the presence of order parameter mixing. These minor peaks in $\rho_{z\pm}(\epsilon)$ vanish eventually as $|\Delta_p|/|\Delta_s|$ is increased toward infinity. Moreover, $\rho_{x,y\pm}(\epsilon)$ (Figs. 3 and 4) are also finite at the bound-state energies. We shall see that the quantization axes for the spins are not aligned with $\hat{z}$. Furthermore, the spin-resolved densities of states are finite also for energies larger than $|\Delta_-|$. This contribution is a continuous (not delta) function in energy, indicating that this contribution to the spin densities and spin currents arises from continuum states not bound near the surface. We note that kinks also appear in these density of states at the gap edges where $\epsilon=\pm|\Delta_\pm|=\pm|\Delta_p\pm\Delta_s|$. In this case, they are $\pm|\Delta_s|$ and $\pm3|\Delta_s|$, respectively.

For a given angle ϕ which parametrizes the quasiparticle path, the surface bound states appear in pairs of equal but opposite energies. The bound-state energy for the $E>0$ branch versus the angle ϕ is plotted in Fig. 5. It can be seen that the Andreev bound states are pushed toward the band edge by the s-wave pairing order parameter. We study in addition (Fig. 5, right panel) the spin polarization $S_i \equiv \frac{\rho_{i,+}-\rho_{i,-}}{\rho_{i,+}+\rho_{i,-}}$ of the Andreev bound state versus the angle ϕ. The sum in the denominator is, in fact, independent of the direction i and equals the density of states. The S_i's in some sense describe the spin direction of the Andreev bounds state.[35] With increasing Δ_p/Δ_s, S_z approaches a step function while S_x approaches zero. Thus we can conclude that the effect of s-wave order parameter is to tilt the spin of Andreev bound states toward the x axis.

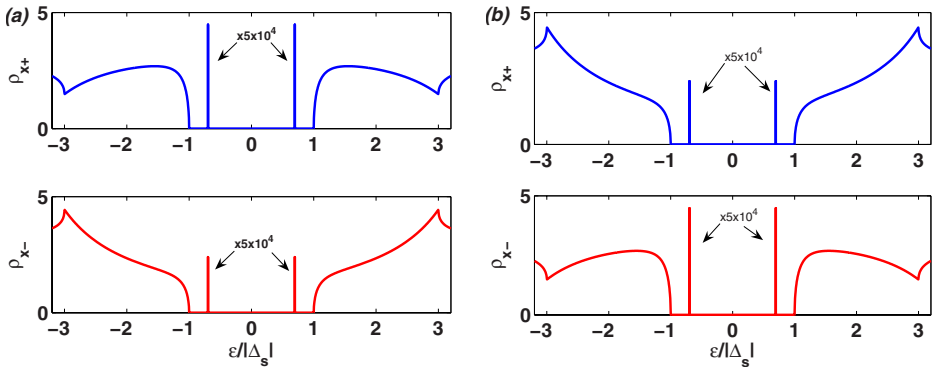

FIG. 3. (Color online) Momentum- and spin-resolved surface densities of states $\rho_{x,\pm}$ in unit of $\frac{N_F}{\pi}$ with $|\Delta_p|=2|\Delta_s|$. (a) $\phi=\frac{\pi}{6}$. (b) $\phi=-\frac{\pi}{6}$. Besides the same symmetry followed by TRS, it shows in additional symmetry with $\epsilon\leftrightarrow-\epsilon$ which forbids the spin current J_y^x.

The spin current density J_y^z at the surface is obtained via the expression

$$J_y^z(x=0)=\frac{\hbar}{2}N_F v_F\int\frac{d\phi}{2\pi}(\sin\phi)T\sum_n \mathrm{Tr}[\sigma^z \underline{g}(\hat{k},\epsilon_n;0)]. \tag{8}$$

The summation over the Matusbara frequency ($T\Sigma_n\mathrm{Tr}[\ldots\underline{g}]$) can be replaced by the integral

$$\int\frac{d\epsilon}{2\pi}\mathrm{Im}\ \mathrm{Tr}[\ldots\underline{g}^{\mathrm{R}}(\epsilon)]\tanh\left(\frac{\epsilon}{2T}\right)$$

with respect to the real frequency ϵ. We shall first note an elementary symmetry relation followed from TRS of our superconducting state

$$\rho_{\hat{n},\pm}(k_y,\epsilon)=\rho_{\hat{n},\mp}(-k_y,\epsilon), \tag{9}$$

which is valid for all spin projections $\hat{n}$. This can be seen in Figs. 2 and 3, etc. From Fig. 2, we see that we also have, in addition, the symmetry $\rho_{z\pm}(k_y,\epsilon)=\rho_{z\pm}(-k_y,-\epsilon)$ [and consequently $\rho_{z+}(k_y,\epsilon)=\rho_{z-}(k_y,-\epsilon)$]. The asymmetry between $\rho_{z+}(k_y,\epsilon)$ and $\rho_{z-}(k_y,\epsilon)$ [and between $\rho_{z+}(k_y,\epsilon)$ and $\rho_{z+}(-k_y,\epsilon)$] causes a finite spin current J_y^z in the topological nontrivial cases as well as in the trivial cases whereas Eq. (9) guarantees that all spin accumulations are zero. For spin projections along $\hat{x}$ and $\hat{y}$ as in Figs. 3 and 4, we have in addition $\rho_{x,y+}(k_y,\epsilon)=\rho_{x,y+}(k_y,-\epsilon)$, (and similarly for $+\rightarrow-$) which forbids both the spin currents J_y^x and J_x^y.

In the trivial Z_2 case where we choose $|\Delta_p|=|\Delta_s|/2$, no subgap state is found as in Fig. 6(a). However, there is still an asymmetry between $\rho_{z+}(k_y,\epsilon)$ and $\rho_{z-}(k_y,\epsilon)$ for the continuum states between the two gaps so that these states continue to contribute to J_y^z. The quasiparticles upon reflection at the surface is now analogous to transmission through a Josephson junction between two unequal-gap SCs with a relative phase difference,[36] where intergap continuum states contribute to a finite current. We suggest here that the contribution to the spin current can be pictured in similar manner. With Eq. (8), we find that J_y^z is indeed nonvanishing. This is justified in the real frequency domain as shown in Fig. 6(b) where a finite contribution to J_y^z is found at energies ϵ between the gaps $-|\Delta_+|<\epsilon<-|\Delta_-|(|\Delta_-|<\epsilon<|\Delta_+|)$. Note that there is no contribution from states with $|\epsilon|>|\Delta_+|$. (These two statements also hold for the topologically nontrivial case.)

In Fig. 7, the values of $J_y^z(x=0)$ as a function of the triplet to singlet order parameter ratio $|\Delta_p|/|\Delta_s|$ is presented. $J_y^z(x=0)$ increases from zero in pure s-wave case toward the value obtained in the pure triplet case. In the topologically trivial regime, $|\Delta_p|<|\Delta_s|$, $J_y^z(x=0)$ seems to be quadric in $|\Delta_p|$ while in the topologically nontrivial regime, it is roughly linearly with $|\Delta_p|$. The asymptotic value for $J_y^z(x=0)$ coincides with our previous results.[23] Figure 8 shows the values of the total spin current $I_y^z\equiv\int_0^\infty dx J_y^z(x)$.

IV. DISCUSSIONS AND CONCLUSIONS

The pairing Hamiltonian can be conveniently written in the helicity basis,[17] $H_\Delta=\frac{1}{2}\Sigma_{\mathbf{k}}(i\Delta_+e^{-i\phi_{\mathrm{k}}}a_{\mathrm{k}+}^\dagger a_{-\mathrm{k}+}^\dagger - i\Delta_-e^{i\phi_{\mathrm{k}}}a_{\mathrm{k}-}^\dagger a_{-\mathrm{k}-}^\dagger)+\mathrm{H.c.}$ Here $\Delta_\pm$ are both real numbers so that the above is time-reversal invariant. ϕ_{k} is the angle between the momentum k and the x axis. The relation $\Delta_{s,p}=(\Delta_+\pm\Delta_-)/2$ can be obtained upon transforming back to the normal spin basis $\{a_{\mathrm{k}\uparrow}^\dagger,a_{\mathrm{k}\downarrow}^\dagger\}$. Thus the pure p-wave Rashba triplet SC and the pure s-wave singlet SC are recovered when $\Delta_+=\mp\Delta_-$, respectively; while the case with $|\Delta_+|\neq|\Delta_-|$ belongs to the NcSC. The nontrivial Z_2 class corresponds to $\Delta_+\Delta_-<0$.[20,21]

The pure s- and p-wave cases, $|\Delta_+|=|\Delta_-|$, are well understood from the previous papers.[23,24] The main difference between the pure triplet case and the present NcSC is that the surface Andreev bound states do not have a fixed spin projection. Moreover, besides the surface bound states, the continuum states between the two gaps, $|\Delta_\pm|$, also contribute to

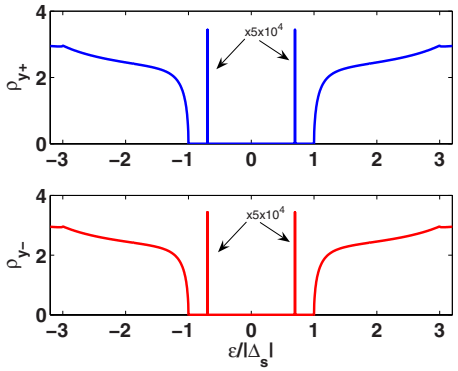

FIG. 4. (Color online) Same as Fig. 3 except here that $\rho_{y,\pm}$ is shown. The results for $\phi=\pm\frac{\pi}{6}$ are identical.

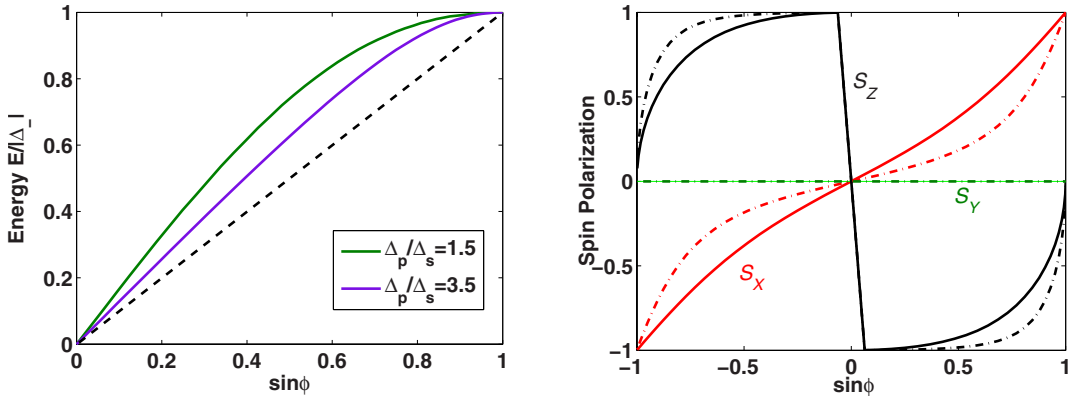

FIG. 5. (Color online) Left: positive energy branch of the surface Andreev bound states, corresponding to the zeros of the anticommutators in Eq. (7), as a function of the angle ϕ for two ratios of Δ_p/Δ_s. The upper (green) and middle (purple) are for the ratios of 1.5 and 3.5, respectively. E is measured in terms of Δ_-. As the triplet component becomes larger, the bound state behaves more like in the pure triplet case where $E=|\Delta_p|\sin\phi$ (the black dashed line). Right: spin polarization of Andreev bound states (defined in text) versus the angle ϕ. Solid lines are for the ratio Δ_p/Δ_s of 1.5 and the dashed ones are for 3.5. The direction of spin polarization evolves in the xz plane as ϕ varies. For smaller angles or larger Δ_p/Δ_s, the bound states are more spin polarized along z as in the pure triplet case.

the spin current and are solely responsible for its nonvanishing value in the topologically trivial case.

In our calculations, where the normal-state spin splitting is not included, only the component J_y^z is nonvanishing while the other components do not appear, even though the quasiparticles have their spins not aligned with the $\hat{z}$ axis. Mixed-parity SC order parameter along with the presence of Rashba spin-orbital interaction accounting for the absence of inversion symmetry may be closer to the physically accessible regime.[22] However, the inclusion can, in principle, generate nonzero spin currents even in the normal-state under equilibrium.[37] Even so, the spin current obtained in the normal state for a spin-split band is *much smaller* than what we have obtained in our mixed-parity superconducting state without the corresponding spin-orbital coupling, provided that the factor $T_c E_F^2/\alpha^3$ is sufficiently large,[24,37] which is presumably true in usual situation when the spin splitting energy $\alpha \ll E_F$. Moreover, inclusion of the spin-orbital coupling in the normal state will make the spin current ill defined because of the lack of spin conservation. In Ref. 24, the authors define the *real* spin current in superconductors by subtracting the contribution obtained in the normal state. They then obtained also finite J_y^x and J_x^y.

In conclusion, we use the exploding-decay tricks to obtain the quasiclassical Green's functions associated with a singlet-triplet mixed noncentrosymmetric superconductor. For the topologically nontrivial NcSC, we obtain a pair of Andreev bound states without a fixed spin projection and a consequent spin current J_y^z. For the topologically trivial NcSC, a finite spin current J_y^z remains even though no Andreev bound state can be found.

ACKNOWLEDGMENTS

This work is supported by the National Science Council of Taiwan.

APPENDIX: EXPLODING AND DECAYING TRICK IN NcSC

Here we shall present our scheme for obtaining the solutions given in Eq. (4) to the Eilenberger equations [Eqs. (1) and (2)] for the NcSC in the presence of a boundary as shown in Fig. 1. Equation (4) is expressed in terms of the exploding and decaying solutions Eqs. (5) and (6) of an auxiliary problem that is identical to the present NcSC for $x>0$. To make our reasoning clearer, we first consider the special case where $\hat{d}$ coincides with $\hat{z}$, then eventually obtain the Green's function for general $\hat{d}$. (A similar method to obtain the quasiclassical Green's function for a uniform noncentrosymmetric superconductor has been also used in Ref. 38. Our treatment extends to the nonuniform case and we

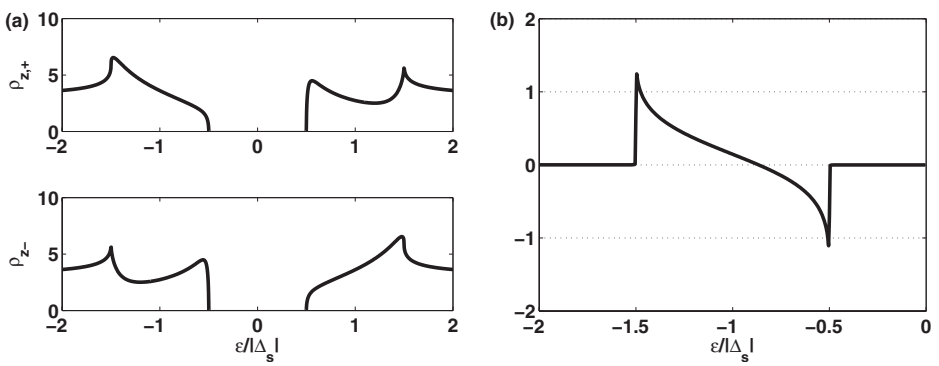

FIG. 6. Topologically trivial NcSC with $|\Delta_p|=0.5|\Delta_s|$. (a) Spin-resolved surface density of states $\rho_{z\pm}$ associated with $k_y=k_F/2$. No subgap states appear. (b) Nonvanishing intergap direction-integrated contributions $\int_0^{\pi/2} d\phi$ $(\sin\phi)\mathrm{Tr}\{\sigma_z\tau_3[-\frac{1}{\pi}\mathrm{Im}\,\hat{g}^R(\epsilon,\phi)]\}$ to J_y^z in the unit of $\hbar v_F N_F|\Delta_s|$.

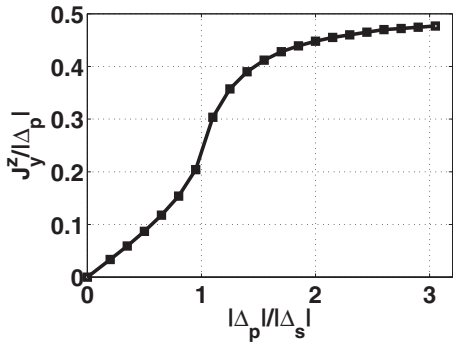

FIG. 7. Surface spin current density J_y^z (in unit of $\hbar v_F N_F |\Delta_p|$) versus the order parameter ratio $|\Delta_p|/|\Delta_s|$ at a temperature $T=|\Delta_s|/100$. In the large $|\Delta_p|$ limit, $J_y^z=\frac{1}{2}\hbar v_F N_F |\Delta_p|$, while the spin current vanishes in the pure singlet case. As $|\Delta_p|$ increases from the topologically trivial to nontrivial regimes, J_y^z follows different dependence on $|\Delta_p|$ around the transition $|\Delta_p|=|\Delta_s|$.

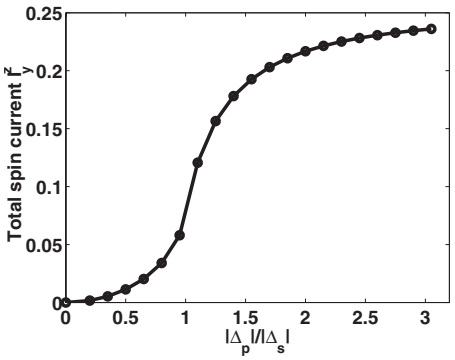

FIG. 8. Total surface spin current density I_y^z (in the unit of $\hbar^2 N_F v_F^2$) versus the order parameter ratio $|\Delta_p|/|\Delta_s|$ at a temperature $T=|\Delta_s|/100$.

also point out some useful mathematical relations not noted in there). The matrix $\hat{M}=(i\epsilon_n-\hat{\Delta})$ appearing in the commutator in Eq. (1) becomes, after an obvious rearrangement of rows and columns, block diagonalized. Explicitly, with $u=\hat{k}\cdot R$, it has the form

$$\left[\begin{pmatrix} \underline{M}^{++} & 0 \\ 0 & \underline{M}^{--} \end{pmatrix}, \begin{pmatrix} \underline{g}^{++} & \underline{g}^{+-} \\ \underline{g}^{+-} & \underline{g}^{--} \end{pmatrix}\right] + iv_F\partial_u \begin{pmatrix} \underline{g}^{++} & \underline{g}^{+-} \\ \underline{g}^{+-} & \underline{g}^{--} \end{pmatrix} = 0, \tag{A1}$$

where the diagonal elements of $\hat{M}$ are

$$\underline{M}^{\pm\pm} \equiv \begin{pmatrix} i\epsilon_n & \mp\Delta_\pm \\ \pm\Delta_\pm^* & -i\epsilon_n \end{pmatrix}. \tag{A2}$$

The parameters $\Delta_\pm=\Delta_s\pm\Delta_p$. By imposing the spatial dependence of $e^{-2\lambda u/v_F}$ to $\hat{g}$, Eq. (A1) becomes a problem for finding eigenvalues λ and the corresponding eigenvectors. For example, the upper diagonal block (++) simplifies to $[\underline{M}^{++},\underline{g}^{++}]-2i\lambda\underline{g}^{++}=0$. This relation is analogous to the pure s- or p-wave cases and can be solved in the same manner. The eigenvalues λ form the set $\{0,0,\alpha_+,-\alpha_+\}$ with $\alpha_+ \equiv \sqrt{\epsilon_n^2+|\Delta_+|^2}$ and the associated eigenvectors are, respectively, the set of 2×2 matrices $\{-i\pi\mathbf{1},\underline{g}_b^{++},\underline{a}_{\alpha_+}^{++},\underline{b}_{-\alpha_+}^{++}\}$. The previous two are the "constant solutions" while $\underline{a}_{\alpha_+}^{++}$ and $\underline{b}_{-\alpha_+}^{++}$ are the decaying and exploding ones, given by

$$\underline{a}_{\alpha_+}^{++} = \begin{pmatrix} -i|\Delta_+|^2 & -\Delta_+(\alpha_+ + \epsilon_n) \\ -\Delta_+^*(\alpha_+ - \epsilon_n) & i|\Delta_+|^2 \end{pmatrix}, \tag{A3}$$

$$\underline{b}_{\alpha_+}^{++} = \begin{pmatrix} i|\Delta_+|^2 & -\Delta_+(\alpha_+ - \epsilon_n) \\ -\Delta_+^*(\alpha_+ + \epsilon_n) & -i|\Delta_+|^2 \end{pmatrix}, \tag{A4}$$

respectively. Besides, the following equality holds as well as in, e.g., Ref. 23

$$\underline{g}_b^{++} = -i\pi[\underline{a}^{++},\underline{b}^{++}]\{\underline{a}^{++},\underline{b}^{++}\}^{-1}, \tag{A5}$$

$$= \frac{-\pi}{\alpha_+}\underline{M}^{++}, \tag{A6}$$

where the subscripts for eigenvalues are omitted if no confusion is generated. Similar results can be obtained in the $(--)$ block by defining $\alpha_-=\sqrt{\epsilon_n^2+|\Delta_-|^2}$. As for the off-diagonal blocks $(+-)$ and $(-+)$, they share the same set of eigenvalues, $\{\pm\alpha_s,\pm\alpha_d\}$, with the subscripts standing for the *sum* and *difference* by $\alpha_{s,d}=\frac{\alpha_+\pm\alpha_-}{2}$. The eigenvectors belonging to the block $(ij)=(+-)$ or $(-+)$ will be labeled as $\{\underline{a}_{\alpha_{s,d}}^{ij},\underline{b}_{\alpha_{s,d}}^{ij}\}$. It should be reminded that the decaying (exploding) solutions are associated with positive (negative) eigenvalues.

Since the product of two solutions to Eq. (A1) also solves that equation, this product must be proportional to another solution, or it must vanish, depending on whether the sum of the corresponding eigenvalues coincides or not with any of the allowed eigenvalues. More precisely, if $\underline{g}_\lambda^{ij}$ is a solution in the (ij) block with eigenvalue λ, then the product $\underline{g}_{\lambda_1}^{ij}\underline{g}_{\lambda_2}^{jk}$ is identical to $\underline{g}_{\lambda_1+\lambda_2}^{ik}$ (up to a proportionality constant) or zero depending on whether $\lambda_1+\lambda_2$ coincides with one of the eigenvalues associated with the block (ik). Using Eq. (A5), the following relations can be easily shown:

$$\underline{a}^{\pm\pm}\underline{g}_b^{\pm\pm} = i\pi\underline{a}^{\pm\pm}, \tag{A7}$$

$$\underline{b}^{\pm\pm}\underline{g}_b^{\pm\pm} = -i\pi\underline{b}^{\pm\pm}, \tag{A8}$$

$$\underline{a}_{\alpha_{d,s}}^{+-}\underline{g}_b^{--} = \mp i\pi\underline{a}_{\alpha_{d,s}}^{+-}, \tag{A9}$$

$$\underline{a}_{\alpha_{d,s}}^{-+}\underline{g}_b^{++} = i\pi\underline{a}_{\alpha_{d,s}}^{-+}, \tag{A10}$$

$$\underline{b}_{\alpha_{d,s}}^{+-}\underline{g}_b^{--} = \pm i\pi\underline{b}_{\alpha_{d,s}}^{+-}, \tag{A11}$$

$$\underline{b}_{\alpha_{d,s}}^{-+}\underline{g}_b^{++} = -i\pi\underline{b}_{\alpha_{d,s}}^{-+}. \tag{A12}$$

Next we return to general $\vec{d}$ direction. Observing that $\underline{g}_b^{\pm\pm}$ in Eq. (A5) can, in fact, be written as $[-\frac{\pi}{\alpha_\pm}\frac{1\pm\sigma_z\tau_3}{2}\hat{M}(\hat{d}=\hat{z})]$ in the 4×4 Nambu notation, we see that the information about $\vec{d}$ is embedded in the projection operator $P_\pm=\frac{1\pm\hat{d}\cdot\hat{\sigma}\tau_3}{2}$, where

$\hat{\sigma} \equiv \{\sigma_x, \sigma_y\tau_3, \sigma_z\}$,[23] and in the order parameter $\hat{\Delta}$ which appears inside $\hat{M}$. From this, we obtain Eqs. (4)–(6). Indeed, it is useful to note that $P_\pm$ commute with $\hat{M}=(i\epsilon_n-\hat{\Delta}_s-\hat{\Delta}_p)$. It is easy to see that $P_\pm\hat{M}$ are the homogeneous solutions to Eq. (1). We can also see that the decaying and exploding solutions in Eqs. (5) and (6) do satisfy Eq. (1), and one can further convince himself/herself by checking the relations, $(\hat{a}^{++})^2=(\hat{b}^{++})^2=(\hat{a}^{--})^2=(\hat{b}^{--})^2=0$, and $(\hat{g}_b)^2=(\hat{g}_b^{++}+\hat{g}_b^{--})^2=-\pi^2$, again hold. By similar reasoning as the $\hat{d}=\hat{z}$ case, Eqs. (A7)–(A12) in the 4×4 form still hold for general $\vec{d}$.

Now we show how the present problem in Fig. 1 can be solved in terms of these auxiliary solutions. For the outgoing path denoted by k, the most general solution with the correct limit as $x\to\infty$ is

$$\hat{g}(u) = \hat{g}_b(k) + c_1^{++}(u)\hat{a}^{++}(k) + c_1^{--}(u)\hat{a}^{--}(k) + c_1^{+-}(u)\hat{a}_{\alpha_s}^{+-}(k) + c_1^{-+}(u)\hat{a}_{\alpha_s}^{-+}(k) \tag{A13}$$

with $u=R\cdot\hat{k}$ positive. For simplicity, the spatial dependence $e^{-2\alpha_+ u/v_F}$ associated with $\hat{a}^{++}$ has been absorbed in the c-number coefficient c_1^{++}, and similarly for the others. For the incoming path,

$$\hat{g}(u) = \hat{g}_b(\underline{k}) + c_2^{++}(u)\hat{b}^{++}(\underline{k}) + c_2^{--}(u)\hat{b}^{--}(\underline{k}) + c_2^{+-}(u)\hat{b}_{\alpha_s}^{+-}(\underline{k}) + c_2^{-+}(u)\hat{b}_{\alpha_s}^{-+}(\underline{k}) \tag{A14}$$

with $u=R\cdot\hat{\underline{k}}$ negative here. We should remark that in the above equations decaying/exploding solutions associated with eigenvalue α_d in the off-diagonal blocks has been excluded. We can see this by two different arguments. First, we can imagine that, far away from the surface, the inversion symmetry is restored. In that case $\alpha_d\to0$ and hence they would become constant solutions, which cannot exist at $x\to\infty$. Second, using relations Eqs. (A7)–(A12), we can check that their appearance would violate the normalization condition in Eq. (2). Now putting $u=0$ in Eq. (A13) and multiplying this equation with $\hat{A}(k)=p_1\hat{a}^{++}+p_2\hat{a}^{--}+p_3\hat{a}_{\alpha_s}^{+-}+p_4\hat{a}_{\alpha_s}^{-+}$, and using Eqs. (A7), (A9), and (A10) yields

$$\hat{A}(k)\hat{g}(0) = i\pi\hat{A}(k), \tag{A15}$$

where the c numbers $\{p_i; i=1,2,3,4\}$ are arbitrary. Similarly, multiplying $\hat{B}(\underline{k})=q_1\hat{b}^{++}+q_2\hat{b}^{--}+q_3\hat{b}_{\alpha_s}^{+-}+q_4\hat{b}_{\alpha_s}^{-+}$ with Eq. (A14) and using Eq. (A8), (A11), and (A12) yields

$$\hat{B}(\underline{k})\hat{g}(0) = -i\pi\hat{B}(\underline{k}), \tag{A16}$$

where again $\{q_i; i=1,2,3,4\}$ are arbitrary. Multiplying the above two equations by $B(\underline{k})$ and $A(k)$, respectively, and add, one obtain the final expression in Eq. (4). The choices for p_i and q_i are not restricted, as long as the anticommutator $\{A(k),B(\underline{k})\}$ has a nonvanishing determinant and hence it is invertible. The determinant vanishes when the energy coincides with the Andreev bound state for a given ϕ, but the invertibility can still be guaranteed by adding a small imaginary number to the energy. Given two sets of matrix, $\hat{A}_1(k)$ and $\hat{B}_1(\underline{k})$, $\hat{A}_2(k)$ and $\hat{B}_2(\underline{k})$ will then yield the same $\hat{g}(0)$. Showing this is quite straightforward if one notices that first, the commutator and the anticommutator in Eq. (4) commute with each other, and second, $\hat{A}_1(k)\hat{A}_2(k)=\hat{B}_1(\underline{k})\hat{B}_2(\underline{k})=0$.

To evaluate the spin current density at a general position x, we need the traces[23] $\mathrm{Tr}[\hat{\sigma}\tau_3\hat{g}(u)]$ at u. If $\hat{d}\|\hat{z}$, we see that contributions to $\mathrm{Tr}[\sigma_z\tau_3\hat{g}(u)]$ arises only from the ++ and −− blocks whereas $\mathrm{Tr}[\sigma_x\tau_3\hat{g}(u)]$ and $\mathrm{Tr}[\sigma_y\hat{g}(u)]$ arise only from the +− and −+ blocks. Hence the latter two have u dependence given by $e^{-2\alpha_s|u|/v_F}$ [see Eqs. (A13) and (A14); note also $\mathrm{Tr}[\hat{\sigma}\tau_3\hat{g}_b]=0$]. Hence for general $\hat{d}$, if $\hat{n}$ is a vector perpendicular to $\hat{d}$, $\mathrm{Tr}[(\hat{n}\cdot\hat{\sigma})\tau_3\hat{g}(u)]$ will have this same u dependence. Since for our superconductor $\hat{d}$ is in the x-y plane, $\mathrm{Tr}[\sigma^z\tau_3\hat{g}(u)]$ is simply $\mathrm{Tr}[\sigma^z\tau_3\hat{g}(0)]e^{-2\alpha_s|u|/v_F}$. The x integral needed for the total spin current is simply $\int_0^\infty dx e^{-2\alpha_s|u|/v_F}=\frac{v_F|\cos\phi|}{2\alpha_s}$.

*chikenl@sfu.ca

[1] B. A. Bernevig, T. L. Hughes, and S. C. Zhang, Science **314**, 1757 (2006).

[2] C. L. Kane and E. J. Mele, Phys. Rev. Lett. **95**, 146802 (2005); **95**, 226801 (2005).

[3] L. Fu, C. L. Kane, and E. J. Mele, Phys. Rev. Lett. **98**, 106803 (2007); L. Fu and C. L. Kane, Phys. Rev. B **76**, 045302 (2007).

[4] M. König, H. Buhmann, W. Molenkamp, T. Hughes, C.-X. Liu, X.-L. Qi, and S.-C. Zhang, J. Phys. Soc. Jpn. **77**, 031007 (2008).

[5] D. Hsieh, Y. Xia, L. Wray, D. Qian, A. Pal, J. H. Dil, J. Osterwalder, F. Meier, G. Bihlmaver, C. L. Kane, Y. S. Hor, R. J. Cava, and M. Z. Hasan, Science **323**, 919 (2009).

[6] Y. Xia, D. Qian, D. Hsieh, L. Wray, A. Pal, H. Lin, A. Bansil, D. Grauer, Y. S. Hor, R. J. Cava, and M. Z. Hasan, Nat. Phys. **5**, 398 (2009).

[7] Y. L. Chen, J. G. Analytis, J.-H. Chu, Z. K. Liu, S.-K. Mo, X. L. Qi, H. J. Zhang, D. H. Lu, X. Dai, Z. Fang, S. C. Zhang, I. R. Fisher, Z. Hussain, and Z.-X. Shen, Science **325**, 178 (2009).

[8] For a recent review, see M. Hasan and C. Kane, arXiv:1002.3895 (unpublished).

[9] N. Read and D. Green, Phys. Rev. B **61**, 10267 (2000).

[10] M. Stone and R. Roy, Phys. Rev. B **69**, 184511 (2004).

[11] For a review on $CePt_3Si$, see E. Bauer, H. Kaldarar, A. Prokofiev, E. Royanian, A. Amato, J. Sereni, W. Brämer-Escamilla, and I. Bonalde, J. Phys. Soc. Jpn. **76**, 051009 (2007).

[12] H. Q. Yuan, D. F. Agterberg, N. Hayashi, P. Badica, D. Vandervelde, K. Togano, M. Sigrist, and M. B. Salamon, Phys. Rev. Lett. **97**, 017006 (2006).

[13] R. Settai, T. Takeuchi, and Y. Ōnuki, J. Phys. Soc. Jpn. **76**, 051003 (2007).

[14] N. Reyren, S. Thiel, A. D. Caviglia, L. Fitting Kourkoutis, G.

Hammerl, C. Richter, C. W. Schneider, T. Kopp, A.-S. Rüetschi, D. Jaccard, M. Gabay, D. A. Muller, J.-M. Triscone, and J. Mannhart, Science **317**, 1196 (2007).
[15] L. P. Gor'kov and E. I. Rashba, Phys. Rev. Lett. **87**, 037004 (2001).
[16] S. K. Yip and A. Garg, Phys. Rev. B **48**, 3304 (1993).
[17] S.-K. Yip, Phys. Rev. B **65**, 144508 (2002); note that there can be other possible broken inversion symmetries, e.g., for O symmetry, see C.-K. Lu and S.-K. Yip, *ibid.* **77**, 054515 (2008).
[18] C.-K. Lu and S.-K. Yip, Phys. Rev. B **78**, 132502 (2008).
[19] Y. Tanaka, T. Yokoyama, A. V. Balatsky, and N. Nagaosa, Phys. Rev. B **79**, 060505(R) (2009).
[20] S.-K. Yip, J. Low Temp. Phys. **160**, 12 (2010).
[21] X.-L. Qi, T. L. Hughes, and S.-C. Zhang, Phys. Rev. B **81**, 134508 (2010).
[22] I. A. Sergienko, Phys. Rev. B **69**, 174502 (2004).
[23] C.-K. Lu and S.-K. Yip, Phys. Rev. B **80**, 024504 (2009).
[24] A. B. Vorontsov, I. Vekhter, and M. Eschrig, Phys. Rev. Lett. **101**, 127003 (2008).
[25] C. Iniotakis, N. Hayashi, Y. Sawa, T. Yokoyama, U. May, Y. Tanaka, and M. Sigrist, Phys. Rev. B **76**, 012501 (2007).
[26] For a recent review, see M. Eschrig, C. Iniotakis, and Y. Tanaka, arXiv:1001.2486 (unpublished).
[27] S. Murakami, N. Nagaosa, and S. C. Zhang, Phys. Rev. Lett. **93**, 156804 (2004).
[28] E. V. Thuneberg, J. Kurkijärvi, and D. Rainer, Phys. Rev. B **29**, 3913 (1984).
[29] M. Fogelström and J. Kurkijärvi, J. Low Temp. Phys. **98**, 195 (1995).
[30] S.-K. Yip, J. Low Temp. Phys. **109**, 547 (1997).
[31] A. L. Shelankov, Sov. Phys. JETP **51**, 1186 (1980); J. Low Temp. Phys. **60**, 29 (1985).
[32] See M. Eschrig, Phys. Rev. B **80**, 134511 (2009), and references therein.
[33] J. W. Serene and D. Rainer, Phys. Rep. **101**, 221 (1983).
[34] P. A. Frigeri, D. F. Agterberg, A. Koga, and M. Sigrist, Phys. Rev. Lett. **92**, 097001 (2004).
[35] We find that the spin polarization obeys $S_x^2+S_z^2=1$ for all angles except at $\phi=0$, where $S_i=0$ for all i as a consequence of the time-reversal invariance of our superconducting state.
[36] L.-F. Chang and P. F. Bagwell, Phys. Rev. B **49**, 15853 (1994); S. K. Yip, *ibid.* **68**, 024511 (2003); S.-T. Wu and S. Yip, *ibid.* **70**, 104511 (2004).
[37] E. I. Rashba, Phys. Rev. B **68**, 241315(R) (2003).
[38] N. Hayashi, K. Wakabayashi, P. A. Frigeri, and M. Sigrist, Phys. Rev. B **73**, 024504 (2006).